CCS Chemistry

RESEARCH ARTICLE

Received: Dec. 26, 2019 | Accepted: Feb. 13, 2020

4-Hydroxy-L-Proline as a General Platform for Stereoregular Aliphatic Polyesters: Controlled Ring-Opening Polymerization, Facile Functionalization, and Site-Specific Bioconjugation

Jingsong Yuan, Dong Shi, Yi Zhang, Jianhua Lu, Letian Wang, Er-Qiang Chen*& Hua Lu*

Beijing National Laboratory for Molecular Sciences, Center for Soft Matter Science and Engineering, Key Laboratory of Polymer Chemistry and Physics of Ministry of Education, College of Chemistry and Molecular Engineering, Peking University, Beijing 100871 (China).

*Corresponding authors: chemhualu@pku.edu.cn, eqchen@pku.edu.cn

Cite this: *CCS Chem.* **2020**, *2*, 236–244

Degradable polyesters have long been regarded as eco-friendly materials, useful for various applications while meeting the growing needs of sustainability. However, it is still challenging to synthesize functional aliphatic polyesters from abundant and cheap renewable sources. Our present study reports a readily available and versatile platform for producing functional and stereoregular aliphatic polyesters from 4-hydroxy-L-proline(4-HYP). We synthesized a bicyclic bridged lactone monomer, namely, N^R-PL, by a simple and scalable two-step process allowing facile side-chain functionalization and derivatization. The ring-opening homopolymerization and copolymerization for the generation of N^R-PL were controlled fully by using organobases such as 1,8-diazabicyclo[5.4.0]-undec-7-ene (DBU) without any detectable epimerization. This process afforded stereoregular polyesters PN^RPE with molar mass (M_n) up to 90 kg/mol and a narrow dispersity ($Đ$) generally below 1.10. The uniqueness of the backbone, which contains two chiral centers on a rigid propyl ring, together with the versatility of the side chain, offer tunable properties complementary to existing aliphatic polyesters. The utility of the polymers was showcased by the facile site-specific bioconjugation of $PN^{EG3}PE$, a water-soluble polyester, to a protein. This work might open numerous opportunities in creating functional and sustainable polyesters for a wide range of applications, including degradable plastics, drug delivery, and protein therapeutics.

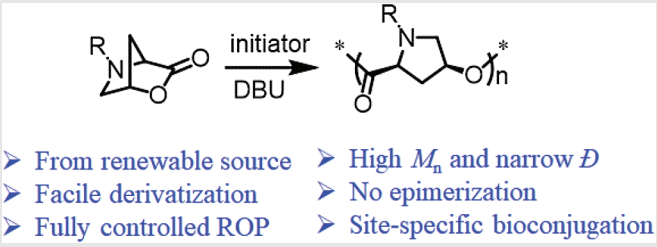

Keywords: 4-hydroxyproline, ROP, sustainable, polyester, stereoregular, bioconjugation

DOI: 10.31635/ccschem.020.201900119
CCS Chem. **2020**, *2*, 236–244

Introduction

The past half-century has witnessed the booming of petroleum-based polymeric materials. However, the everlasting life span and end-of-use issues of such plastics have caused vast environmental pollutions, making sustainable polymeric products derived from renewable feedstock increasingly desirable.[1-10] Degradable aliphatic polyesters have long been regarded as eco-friendly materials useful for various applications, including food packing, containers, agricultural mulching film, and biomaterials.[5,11] For instance, polylactide (PLA), produced by the ring-opening polymerization (ROP) of lactide, is an excellent material for surgical suturing and disposable packing owing to its biocompatibility, biodegradability, and mechanical properties.[12-14] Additionally, polyhydroxyalkanoates (PHA) such as poly(3-hydroxybutyrate) (P3HB) either biosynthesized using fermentation or chemically synthesized via the ROP of lactones, have long been considered promising candidates for substituting petroleum-based plastics.[15,16] Despite the immense promises, the current choices of bio-renewable aliphatic polyesters are still rare; therefore, there is a pressing need for an expanded repertoire of functionalizable polyesters.[17-23] Accordingly, the recent development of the ROP of amino acid-derived *O*-carboxyanhydride (OCA) has gained considerable success in preparing functional poly(α-hydroxy acid)s.[24-27] However, the handling of OCA requires sophisticated synthetic skills, in the sense that, α-amino acids need to be converted into their corresponding α-hydroxyl acids before the transformation into the unstable OCA monomers under anhydrous conditions. Moreover, the ROP of OCAs often leads to racemization due to the enhanced acidity of α-hydrogen, which was addressed only recently by using carefully designed organometallic or organic catalysts.[26,28-30] As such, a novel monomer platform that could provide easier access to libraries of functional and stereoregular polyesters from bio-derived resources is still an urgent need.

4-Hydroxyl-L-proline (4-HYP) is abundant in collagen and many other proteins; it is a naturally occurring amino acid conveniently accessible at relatively low prices. Previously, 4-HYP-based polyesters with only low molar mass (M_n), typically < 12 kg·mol^{-1}, and broad dispersity ($Đ$) > 1.5, were reported by Langer et al.[31,32] and Park et al.[33] by step-growth condensation polymerization, whereas a well-controlled ROP process has never been reported. We envisioned that 4-HYP is an ideal building block to construct functional polyesters via ROP approach for the following reasons: (1) 4-HYP could be convert readily to a bicyclic bridged lactone, namely N^R-PL (Scheme 1), with the amine group as a convenient chemical handle for functionalization by using a well-established protocol.[34] (2) In general, the α-hydrogen of α-amino acids is less acidic, compared with α-hydroxyl acids due to a weaker induction effect, thus making epimerization less likely. (3) Recently, we showed that 4-HYP-derived bridged bicyclic thiolactones (N^R-PTL) could undergo well-controlled ROP and afford high M_n and narrow $Đ$ polythioesters.[35] The control over ROP was achieved through the judicious molecular design, which involved highly strained monomers for rapid chain propagation and inert proline–proline thioester junctions in the polymer backbone for minimized chain transfer.[36] Owing to the structural similarity, we speculated that N^R-PL might also generate an outstandingly controlled ROP, thereby, representing a modulable platform for fabricating numerous functional, sustainable polyesters with tunable properties.

Results and Discussion

Synthesis and controlled ROP of N^R-PL

As depicted in Scheme 1, various alcohols were coupled to the amino group of 4-HYP through a urethane group. Next, the precursors N^R-HYP were converted to corresponding monomers bearing different side chains via Mitsunobu reaction with typical yields ~53–80%.[34]

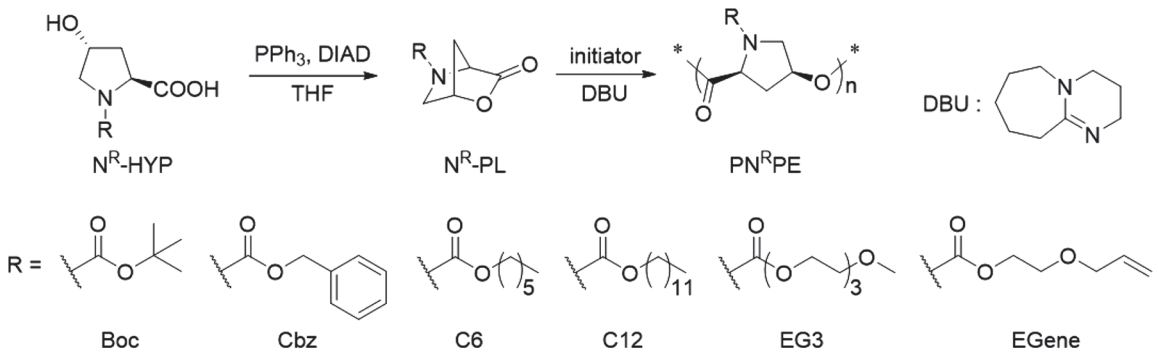

Scheme 1 | *Synthesis and ring-opening polymerization of a bicyclic bridged lactone monomer, N^R-PL, for the subsequent fabrication of functional, stereoregular aliphatic polyesters.*

DOI: 10.31635/ccschem.020.201900119
CCS Chem. **2020**, *2*, 236–244

N^{Boc}-PL, N^{C6}-PL, and N^{C12}-PL were selected as monomers bearing alkyl side chains of varying lengths and branching degrees; N^{Cbz}-PL, N^{EG3}-PL, and N^{EGene}-PL were synthesized to represent monomers carrying aryl, hydrophilic, and modifiable moieties, respectively. The characterization data of the precursors and monomers were obtained by ^{1}H, ^{13}C nuclear magnetic resonance (NMR), ^{1}H–^{13}C heteronuclear single quantum coherence (HSQC) NMR, and single-crystal X-ray diffraction (XRD), compiled in Supporting Information Figures S1–S21.

We started our ROP investigation by screening proper organobases for the monomer N^{C12}-PL using benzyl alcohol as a model initiator. We found that weak bases such as triethylamine (TEA), did not lead to any monomer conversion (entry 1, Supporting Information Table S1). Some phosphazene bases, such as 2-*tert*-butylimino-2-diethylamino-1,3-dimethylperhydro-1,3,2-diazaphosphorine (BEMP; BEMP–H^+ $pK_a^{MeCN} = 27.6$) and the cyclic trimeric phosphazene base (CTPB; CTPB–H^+, $pK_a^{MeCN} = 33.3$), gave fast ROP and over 95% monomer conversion in tetrahydrofuran (THF).[37] However, both phosphazene superbases mediated ill-controlled ROP, as revealed by multimodal peaks, low M_n, and broad $Đ$ in size-exclusion chromatography (SEC; entries 2 and 3, Supporting Information Table S1). In contrast, when the base 1,8-diazabicyclo[5.4.0]-undec-7-ene (DBU, DBU–H^+ $pK_a^{MeCN} = 24.3$) was used for the ROP at an initial monomer/initiator/base ratio ($[M]_0/[I]_0/[base]_0$) of 50/1/1 in deuterated chloroform ($CDCl_3$), a > 95% monomer conversion was realized within 24 h, affording poly(*N*-carboxydodecane 4-hydroxyl-L-prolyl ester) ($PN^{C12}PE$) with a sharp and unimodal peak in SEC. Also, the ROP was confirmed by ^{1}H NMR spectroscopy (Supporting Information Figure S22), and the shift of the ester carbonyl stretch peak from 1800 cm^{-1} of the lactone to the corresponding 1748 cm^{-1} of the open-chain ester was demonstrated by Fourier-transform infrared (FT-IR) spectroscopy (Supporting Information Figure S23). The M_n and $Đ$ measurements obtained were 17.9 $kg{\cdot}mol^{-1}$ (expected $M_n = 16.3$) and 1.09, respectively (entry 1, Table 1). Notably, prolonging the reaction time to 72 h did not cause broadening of the peak in the SEC, suggesting minimal transesterification-induced chain transfer, even after monomer consumption. Besides, increasing the equivalent of DBU to $[M]_0/[I]_0/[base]_0$ = 50/1/5 led to a significantly enhanced ROP rate (> 95% monomer conversion within 5 h) without jeopardizing the degree of control of the reaction (entry 2, Table 1).

Table 1 | *Ring-Opening Polymerization Results of N^R-PL[a] Formation*

Entry	Monomer	$[M]_0/[I]_0/[base]_0$	Solvent	Time (h)	M_n^{cal} ($kg{\cdot}mol^{-1}$)[b]	M_n^{obt} ($kg{\cdot}mol^{-1}$)[c]	$Đ$[e]
1	N^{C12}-PL	50/1/1	$CDCl_3$	24	16.3	17.9	1.09
2	N^{C12}-PL	50/1/5	$CDCl_3$	5	16.3	17.0	1.07
3	N^{C12}-PL	50/1/5	DCM	4	16.3	14.0	1.10
4	N^{C12}-PL	50/1/5	THF	24	16.3	17.9	1.11
5	N^{C12}-PL	25/1/5	$CDCl_3$	2	8.1	8.0	1.06
6	N^{C12}-PL	75/1/5	$CDCl_3$	8	24.4	21.8	1.08
7	N^{C12}-PL	100/1/5	$CDCl_3$	12	32.5	29.8	1.06
8	N^{C12}-PL	150/1/5	$CDCl_3$	18	48.8	48.4	1.09
9	N^{C12}-PL	200/1/5	$CDCl_3$	30	65.0	58.9	1.12
10	N^{C12}-PL	300/1/5	$CDCl_3$	48	97.5	89.6	1.18
11	N^{C6}-PL	50/1/5	$CDCl_3$	5	12.1	9.9	1.06
12	N^{C6}-PL	100/1/5	$CDCl_3$	12	24.1	21.2	1.08
13	N^{EG3}-PL	25/1/5	$CDCl_3$	2	7.6	7.1[d]	1.09
14	N^{EG3}-PL	50/1/5	$CDCl_3$	5	15.2	14.1[d]	1.06
15	N^{EG3}-PL	75/1/5	$CDCl_3$	8	22.7	19.3[d]	1.09
16	N^{EGene}-PL	25/1/1	$CDCl_3$	10	6.0	6.1[d]	1.08
17	N^{Boc}-PL	50/1/1	$CDCl_3$	24	10.6	13.4[d]	1.05
18	N^{EG3}-PL-*r*-N^{Cbz}-PL	25/25/1/5	$CDCl_3$	5	13.8	13.0[d]	1.05
19	N^{EG3}-PL-*b*-N^{C12}-PL	25/25/1/5	$CDCl_3$	2/2	15.7	14.6	1.09

[a] All the polymerizations were conducted at 25 °C in a glove box with benzyl alcohol as the initiator, DBU as the base, $[N^R\text{-PL}]_0 = 1.4$ M, quenched upon >95% monomer conversion.
[b] Calculated molar mass based on feeding $[M]_0/[I]_0$ ratio.
[c] Obtained relative molar mass determined by SEC in THF using polystyrene as the standard; $PN^{C6}PE$ and $PN^{C12}PE$ were insoluble in DMF.
[d] Obtained absolute molar mass determined by SEC in DMF containing 0.1 M LiBr equipped with a multiangle laser light scattering (MALLS) detector.
[e] Dispersity, determined by SEC.

DOI: 10.31635/ccschem.020.201900119
CCS Chem. **2020**, *2*, 236–244

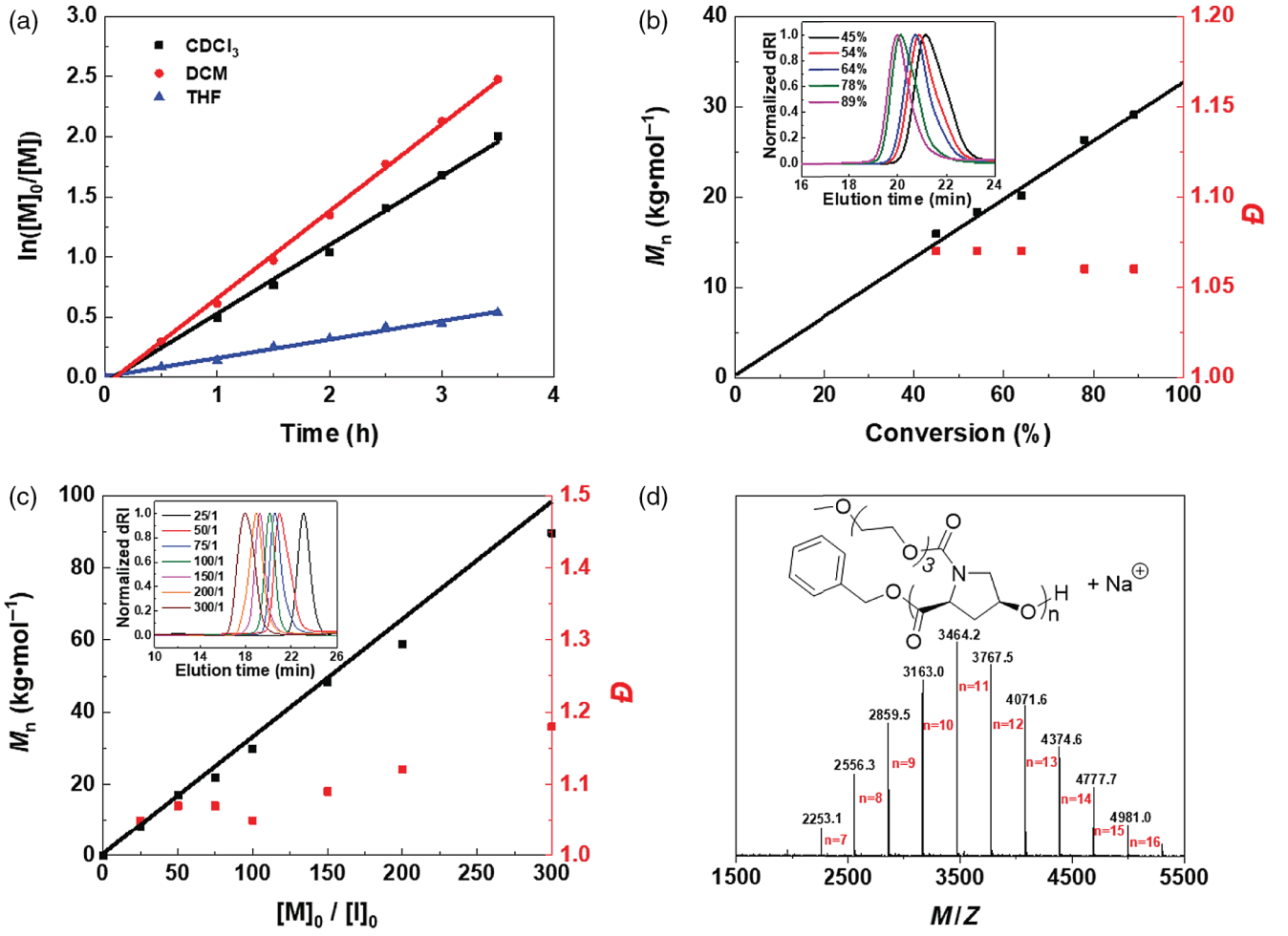

Figure 1 | *Controlled ROP of N^R-PL. (a) ln([M]$_0$/[M]) as a function of time for the N^{C12}-PL ROP in different solvents at 30 °C, [M]$_0$/[I]$_0$/[base]$_0$ = 50/1/5. (b) The plots of M_n and Đ as a function of monomer conversion for the N^{C12}-PL ROP at 25 °C, [M]$_0$/[I]$_0$/[base]$_0$ = 100/1/5. Inset: overlay of SEC traces at different monomer conversions. (c) The plots of M_n and Đ as a function of feeding [M]$_0$/[I]$_0$ ratio for N^{C12}-PL ROP. Inset: overlay of SEC traces at different [M]$_0$/[I]$_0$ ratios. (d) MALDI-TOF mass spectrum of $PN^{EG3}PE$ initiated by benzyl alcohol, [M]$_0$/[I]$_0$/[base]$_0$ = 10/1/5. ROP, ring-opening polymerization; N^R-PL, a bicyclic bridged lactone monomer; SEC, size-exclusion chromatography; MALDI-TOF, matrix-assisted laser desorption/ionization-time of flight.*

Further, DBU-mediated ROP in other common organic solvents, such as dichloromethane (DCM) and THF, also gave similar well-controlled results (entries 3 and 4, Table 1; Supporting Information Figure S24). Kinetic studies of the DBU-catalyzed ROPs depicted first-order kinetics over monomer concentration in all three solvents, with those in DCM and $CDCl_3$ being considerably faster than that in THF (Figure 1a). Moreover, the well-controlled chain-growth feature of DBU-mediated ROP of N^{C12}-PL was confirmed by the linear relationship of M_n with the monomer conversion (Figure 1b) or the feeding [M]$_0$/[I]$_0$ ratio (Figure 1c). SEC analyses exhibited sharp and narrow unimodal peaks for all the polymers (inset of Figure 1b and c). The M_n of $PN^{C12}PE$ obtained were in < 10% deviation from expected values, and Đ were in the range of 1.06–1.18 (entries 5–10, Table 1). The highest M_n of $PN^{C12}PE$ obtained in this study was 89.6 kg·mol^{-1} at a feeding [M]$_0$/[I]$_0$ ratio of 300/1.

To expand the monomer scope, we explored the ROP of N^{Boc}-PL, N^{Cbz}-PL, N^{C6}-PL, N^{EG3}-PL, and N^{EGene}-PL, respectively, under the reaction conditions mentioned above. Four out of the five monomers, namely N^{Boc}-PL, N^{C6}-PL, N^{EG3}-PL, and N^{EGene}-PL gave over 95% conversion and controlled the homopolymerization process satisfactorily (entries 11–17, Table 1; Supporting Information Figures S25–S29). For example, N^{EG3}-PL was polymerized in a fully controlled manner and gave water-soluble $PN^{EG3}PE$ with linear growth of M_n as a function of feeding [M]$_0$/[I]$_0$ ratio up to 75/1 as unimodal SEC peaks (Supporting Information Figure S30). Matrix-assisted laser desorption ionization-time of flight mass spectrometry (MALDI-TOF MS) of benzyl alcohol-initiated ROP of N^{EG3}-PL at a

DOI: 10.31635/ccschem.020.201900119
CCS Chem. **2020**, *2*, 236–244

feeding $[M]_0/[I]_0$ ratio of 10/1 displayed a group of Poisson-distributed peaks, which were assigned to oligomeric PN^{EG3}PE bearing the $C_6H_5CH_2$–/–OH end groups (Figure 1d). Homopolymerization of N^{Cbz}-PL in most common organic solvents, including DCM, $CDCl_3$, THF, and DMF, led to evident precipitation due to the poor solubility of resultant PN^{Cbz}PE. Nevertheless, a random copolymerization of N^{EG3}-PL and N^{Cbz}-PL gave copolymers with good solubility and excellent control, shown by both M_n and $Đ$ (entry 18, Table 1). Sequential ROP of N^{EG3}-PL and N^{C12}-PL in one-pot synthesis gave a well-defined block copolymer P(N^{EG3}PE-*b*-N^{C12}PE), once again highlighting the controllability of the ROP (entry 19, Table 1; Supporting Information Figure S31). Moreover, the structural diversity of the polymer was tailorable by postpolymerization modification of PN^{EGene}PE via highly efficient UV-triggered thiol–ene reaction, which enabled the facile introduction of cationic, anionic, as well as zwitterionic moieties in an almost quantitative fashion (Supporting Information Figures S32–S35). Overall, the ROP of N^{R}-PL offered outstanding control and tunability over M_n, $Đ$, end groups, and side-chain functionalities.

Stereoregularity of PN^{R}PE

The ROP of OCA could undergo epimerization easily due to the deprotonation of the acidic α-hydrogen. Thus, we conducted comprehensive NMR and hydrolysis studies to investigate the stereoregularity of N^{R}-PL ROP (Figure 2). Unfavorably, ^{13}C NMR spectrum of PN^{Boc}PE in $CDCl_3$ at room temperature (Figure 2a) exhibited complicated splitting and multimodal peaks. Switching the solvent to DMF-d_7, the same polymer gave a considerably cleaner ^{13}C NMR spectrum pattern than that in $CDCl_3$ (Figure 2a), but the peaks for carbon (*c*, *d*, and *b*) were still broad and difficult to assign. We reasoned that the broadening and splitting could be a combined effect of the *trans*–*cis* isomerization of the urethane carbonyl and the *endo*–*exo* conformation isomerization of the prolyl ring.[38–40] This notion was later confirmed by the ^{13}C NMR spectroscopy measurements of PN^{Boc}PE in DMF-d_7 at 90 °C, which showed sharp and single peaks for major prolyl carbons (Figure 2a). We next hydrolyzed the monomer N^{EG3}-PL and corresponding polymer PN^{EG3}PE in alkaline D_2O solution at 4 °C for 2 h to obtain more conclusive evidence regarding the tacticity of the polymers. Interestingly, completion of both hydrolysis reactions were attained, giving almost identical ^{1}H NMR spectra, assignable to the pure enantiomer (2*S*,4*S*)-*N*-(2,5,8,11-tetraoxadodecanoyl)-4-hydroxypyrrolidine-2-carboxylic acid (top and middle spectra in Figure 2b), which was distinct from the ^{1}H NMR of (2*S*,4*R*)-*N*-(2,5,8,11-tetraoxadodecanoyl)-4-hydroxypyrrolidine-2-carboxylic acid (*trans*-N^{EG3}-HYP; bottom spectrum in Figure 2b). Together, we inferred from the solvent and temperature-dependent ^{13}C NMR spectroscopy and the ^{1}H NMR analysis of the hydrolysis product that there was indeed no epimerization during the polymerization process.

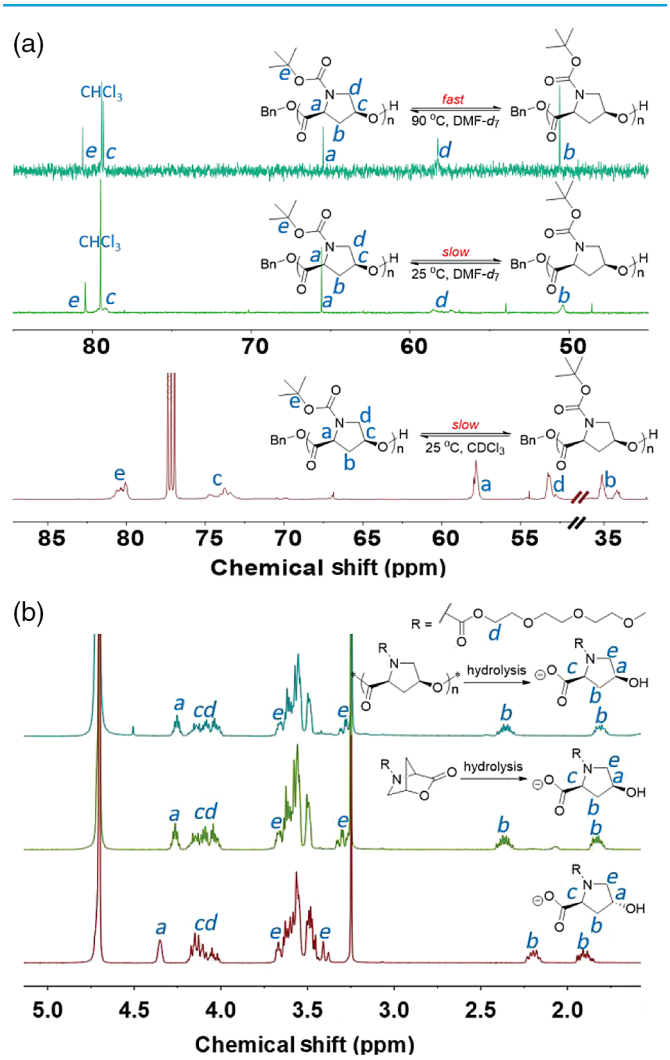

Figure 2 | *(a) Overlay of ^{13}C NMR spectra of PN^{Boc}PE in $CDCl_3$ (25 °C) and DMF-d_7 (25 and 90°C). (b) Overlay of ^{1}H NMR spectra of* trans-*N^{EG3}-HYP and the hydrolyzed product of N^{EG3}-PL and PN^{EG3}PE in alkaline D_2O (pD = 10 for N^{EG3}-PL pD = 13 for PN^{EG3}PE, respectively, 4 °C, 2 h).*

Thermal and mechanical properties of PN^{R}PE

We conducted thermogravimetric analysis (TGA) and differential scanning calorimetry (DSC) experiments to evaluate the thermal property and phase transition of PN^{R}PE. The decomposition temperature (T_d) to a 5% weight loss of PN^{EG3}PE, PN^{C6}PE, and PN^{C12}PE were ~300 °C, close to the T_d of most aliphatic polyesters, while the T_d of PN^{Boc}PE and PN^{EGene}PE were 210 °C and 252 °C, respectively, likely due to the thermal instability of the Boc and allyl carbamate groups (Supporting Information Figure S36 and Supporting Information Table S2). The DSC traces acquired during the second

DOI: 10.31635/ccschem.020.201900119
CCS Chem. **2020**, *2*, 236–244

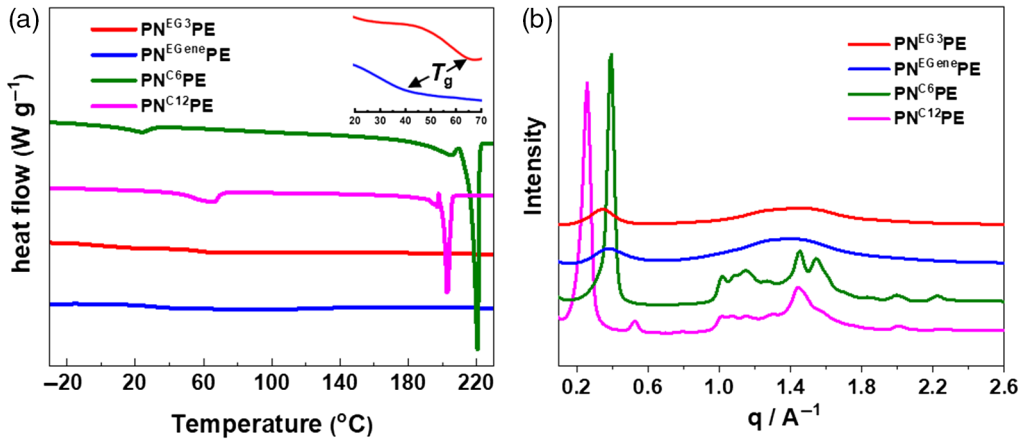

Figure 3 | *(a) DSC traces of PN^{R}PE obtained during the second heating at a rate of 10 °C/min; Inset: expanded DSC traces of PN^{EG3}PE and PN^{EGene}PE demonstrating the glass transformation. (b) One-dimensional-XRD profiles of PN^{R}PE recorded at room temperature. DSC, differential scanning calorimetry; PN^{R}PE, bicyclic bridged lactone monomer.*

heating at a rate of 10 °C/min of PN^{R}PE are depicted in Figure 3a. The glass transition temperatures (T_g) of PN^{EG3}PE and PN^{EGene}PE were detected at 40 °C and 64 °C, respectively. PN^{C12}PE and PN^{C6}PE showed complex transition behaviors; in the low-temperature range, both samples likely underwent the glass transition immediately, followed by a cold-crystallization process, resulting in an overall apparent endothermic process. Moreover, upon heating PN^{C12}PE to high temperature (190 °C), sequential small endotherm, an exotherm, and a larger endotherm were observed, suggesting a minor melting/recrystallization at 196 °C and 198 °C, respectively occurred, proceeded by a major melting process with a melting temperature (T_m) at 202 °C. For PN^{C6}PE, the larger endothermic peak was apparent at 221 °C, right after the small one at 206 °C. The DSC results implied that PN^{C12}PE and PN^{C6}PE might exhibit crystalline phase at low temperatures, and can be fabricated into a transparent film by hot compression at 180 °C (Supporting Information Figure S37). Besides, the strain–stress curve of PN^{C12}PE revealed a 6.1% elongation at break and Young's modulus of 143 MPa at 20°C (Supporting Information Figure S38).

Figure 3b depicted the one-dimensional (1D) XRD profiles of PN^{R}PE in which the samples were cooled at 1.0 °C/min from the molten state to room temperature. The XRD results indicated that both PN^{EG3}PE and PN^{EGene}PE were amorphous, in agreement with the DSC results. Two scattering halos were observed in the low- and high-angle regions, of which the former was believed to associate with the lateral dimension of the chain bearing rigid backbone and the relatively large pendants. In contrast, both PN^{C12}PE and PN^{C6}PE showed several sharp diffraction peaks. For PN^{C12}PE, three low-angle peaks following a ratio of scattering vector (q-ratio) of 1:2:3 were detected, with the first peak at 0.260 Å^{-1}. This observation was an indication of a layer structure with a layer period of 24.2 Å. Similar low-angle diffraction was observed with PN^{C6}PE, having a shorter side chain of hexyl, and presenting a smaller layer period of 15.8 Å. In the high-angle region, PN^{C12}PE and PN^{C6}PE showed similar diffraction patterns, confirming the existence of crystalline structures. The crystallization behaviors were different between PN^{EG3}PE, PN^{EGene}PE and PN^{C12}PE, PN^{C6}PE, which might result from the differences in both their main-chain and side-chain compatibility. Collectively, the above results suggested that the thermal and mechanical properties of PN^{R}PE could be tailored readily in a broad range by simply adjusting the side chains, thereby, offering tremendous potential for materials optimization in the future.

Site-specific protein conjugation

Previously, we employed trimethylsilyl phenylsulfide as an initiator for the ROP of amino acid *N*-carboxyanhydride (NCA) to install in situ a reactive phenyl thioester group at the end of synthetic polypeptides. Then the polymers were attached to enhanced green fluorescent protein bearing an *N*-terminal Cysteine (Cys-eGFP) successfully via a chemoselective native chemical ligation (NCL).[41,42] Here, we envisaged that a similar strategy could be applicable for protein–PN^{EG3}PE conjugation if a phenyl thioester could be installed at the α-chain end of PN^{EG3}PE (Figure 4a). For this reason, thiophenol and DBU were selected to mediate the ROP of N^{EG3}-PL simultaneously, which afforded PN^{EG3}PE bearing terminal phenyl thioester (PN^{EG3}PE-SPh) with a M_n of 6.0 kg·mol^{-1} and a $Đ$ of 1.07 in SEC (Supporting Information Figure S39). Remarkably, MALDI-TOF MS analysis of PN^{EG3}PE-SPh revealed exclusively, the corresponding oligomer bearing the desirable phenyl thioester group on the chain end (Figure 4b). Next,

DOI: 10.31635/ccschem.020.201900119
CCS Chem. **2020**, *2*, 236–244

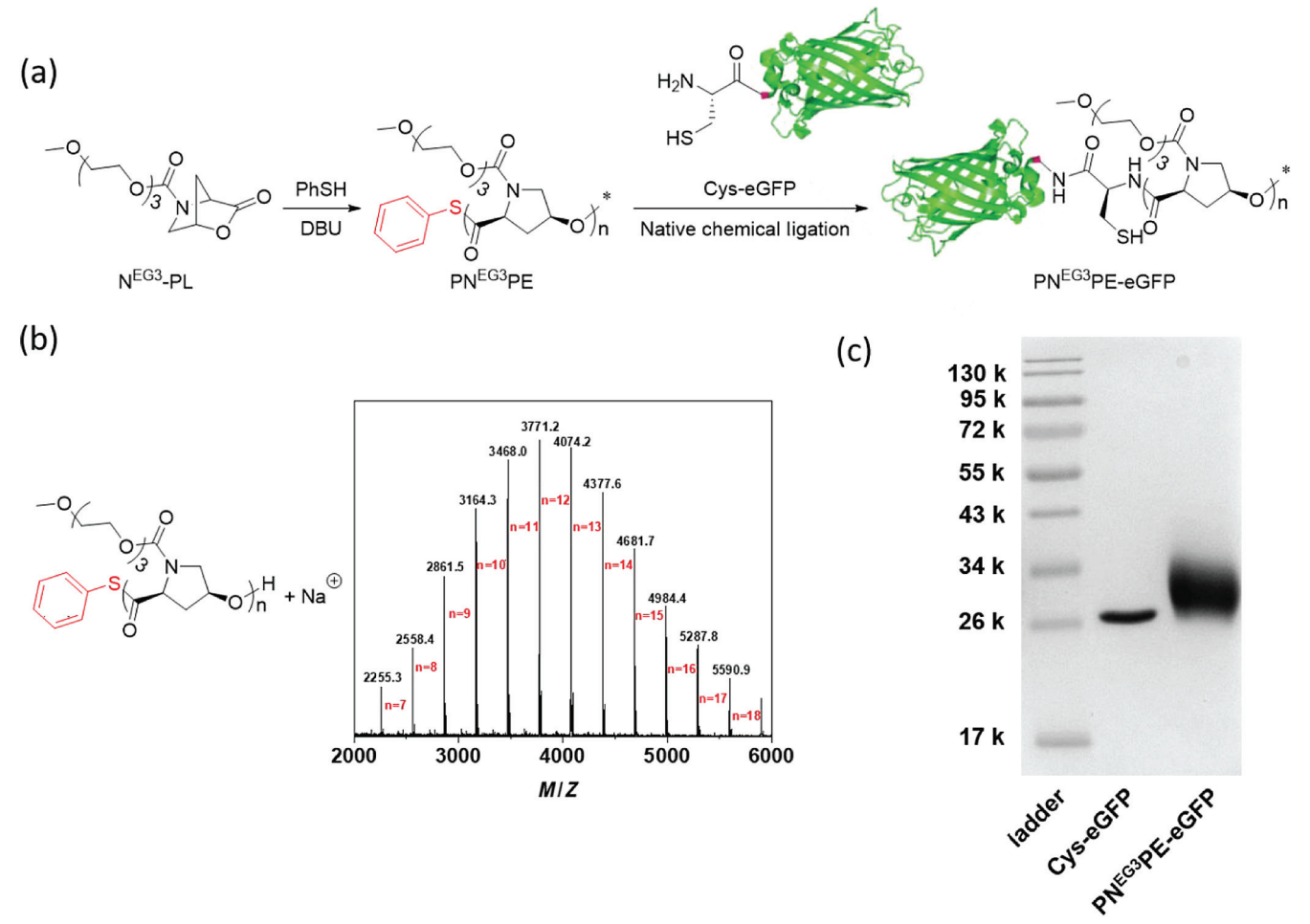

Figure 4 | *(a) Synthesis of PN^{EG3}PE-SPh and subsequent NCL reaction with Cys-eGFP. (b) MALDI-TOF mass spectrum of PN^{EG3}PE initiated by thiophenol, $[M]_0/[I]_0/[base]_0 = 10/1/1$. (c) SDS-PAGE of PN^{EG3}PE-eGFP conjugate. NCL, native chemical ligation; Cys-eGFP, cysteine-rich tagged green fluorescent protein MALDI-TOF; matrix-assisted laser desorption/ionization-time of flight.*

we pursued the conjugation of PN^{EG3}PE-SPh to a Cys-eGFP. Room temperature incubation of the two substrates at a molar ratio of 3/1 in 50 mM Tris·HCl buffer (pH = 7.0) for 12 h, afforded a 90% Cys-eGFP conversion (Supporting Information Figure S40) and a purification yield of 47% of the corresponding conjugate, PN^{EG3}PE-eGFP (Figure 4c). It is noteworthy that alkyl prolyl thioester was notoriously sluggish in NCL. Nonetheless, by using an *in situ* installed phenyl prolyl thioester, we demonstrated that effective NCL could take place at a reasonably good rate and yield without additives or catalysts promotion.

Experimental Methods

General procedure for the synthesis of N^{R}-PL

We present N^{C12}-PL as a model for the synthesis reaction, as follows: A solution of diisopropyl azodicarboxylate (DIAD; 4.1 g, 20.4 mmol, 1.1 equiv.) dissolved in THF (40 mL) was added dropwise to a solution mixture of N^{C12}-HYP (6.4 g, 18.5 mmol, 1.0 equiv.) and triphenylphosphine (5.3 g, 20.4 mmol, 1.1 equiv.) dissolved in THF (250 mL) over 20 min period at 0°C. Subsequently, the reaction was stirred at room temperature for 4 h, following solvent removal by rotary evaporation. We purified the crude product by column chromatography (DCM:EA = 40:1) to afford a white solid (4.5 g, yield 74%). The conditions for the crystal characterization and the results are indicated, as follows: ^{1}H NMR (400 MHz, $CDCl_3$): δ 5.11 (s, 1H), 4.61 (br, 1H), 4.12 (t, J = 6.7 Hz, 2H), 3.59 (d, J = 10.8 Hz, 1H), 3.50 (d, J = 10.6 Hz, 1H), 2.24 (d, J = 10.8 Hz, 1H), 2.03 (d, J = 10.6 Hz, 1H), 1.64 (m, 2H), 1.26 (m, 18H), 0.88 (t, J = 6.6 Hz, 3H). ^{13}C NMR (126 MHz, $CDCl_3$): δ 170.7, 154.7, 78.3, 66.3, 57.4, 50.0, 39.1, 31.9, 29.6, 29.5, 29.3, 29.2, 28.9, 25.8, 22.7, 14.1. Electrospray ionization mass spectrometry (ESI-MS): Calculated m/z = 325.2; found m/z = 348.1 $[M + Na]^+$.

DOI: 10.31635/ccschem.020.201900119
CCS Chem. **2020**, *2*, 236–244

General procedure for the ROP of N^R-PL

We use N^{C12}-PL as an example for the ROP, as follows: In a glovebox, the solution of N^{C12}-PL (32.5 mg, 0.1 mmol, 50 equiv.) in $CDCl_3$ (22 μL) was mixed with benzyl alcohol (2.0 μL × 1.0 M, 1.0 equiv.) in $CDCl_3$, followed by the addition of 1,8-Diazabicyclo[5.4.0]undec-7-ene (DBU; 10.0 μL × 1.0 M, 5.0 equiv.) in $CDCl_3$, and stirring the reaction at room temperature for 5 h. Then an aliquot of the solution was quenched by acetic acid (10.0 μ × 1.0 M) in $CDCl_3$ before analysis by ^{1}H NMR for the calculations of the monomer conversion. The polymer was purified initially by precipitation in hexane (10 mL) and centrifuged (4000 g for 5 min). After drying, the average yield obtained was ~ 80–90%. The polymer was characterized as follows: M_n and $Đ$ were measured by size-exclusion chromatography (SEC). ^{1}H NMR (400 MHz, $CDCl_3$): δ 7.38 (br, 0.11H), 5.24 (br, 1H), 4.86–4.35 (m, 1H), 4.25–3.90 (m, 2H), 3.85–3.47 (m, 2H), 2.80–2.22 (m, 2H), 1.61 (br, 2H), 1.26 (br, 18H), 0.88 (m, 3H).

Conclusions

We have demonstrated here the facile synthesis of a series of 4-HYP-derived functional aliphatic polyesters, (N^R-PL), bearing tunable side chains. The polymerization process of the N^R-PL was carefully controlled by using DBU as the catalyst and alcohol/thiol as initiators, affording stereoregular PN^RPE polyesters with controlled M_n up to ~90 kg·mol^{-1} and well-defined end groups. The solubility and thermomechanical properties of the resulting PN^RPE were tailored easily by the introduction of side-chain functionalization either directly from the monomer or indirectly via postpolymerization modification. One polymer, $PN^{EG3}PE$, demonstrated excellent water solubility and was amenable to site-specific protein conjugation via highly efficient NCL. With the controlled ROP and tunability of N^R-PL, this approach has the potential to open opportunities in creating functional polyesters from renewable sources for a wide range of applications, including special plastics, drug delivery, and protein therapeutics.

Supporting Information

Supporting Information is available.

Conflicts of Interest

There is no conflict of interest to report.

Acknowledgments

We thank Prof. Eugene Y.-X. Chen, Prof. Zi-Chen Li, Prof. Youhua Tao, and Prof. Rong Tong for inspiring discussions. This research was made possible as a result of a generous grant from the National Natural Science Foundation of China (21722401 for H. Lu and 21634001 for E.Q. Chen).

References

1. Schneiderman, D. K.; Hillmyer, M. A. 50th Anniversary Perspective: There Is a Great Future in Sustainable Polymers. *Macromolecules* **2017**, *50*, 3733–3749.
2. Hong, M.; Chen, E. Y. X. Chemically Recyclable Polymers: A Circular Economy Approach to Sustainability. *Green Chem.* **2017**, *19*, 3692–3706.
3. Lu, X. B.; Liu, Y.; Zhou, H. Learning Nature: Recyclable Monomers and Polymers. *Chemistry* **2018**, *24*, 11255–11266.
4. Zhu, Y.; Romain, C.; Williams, C. K. Sustainable Polymers from Renewable Resources. *Nature* **2016**, *540*, 354–362.
5. Tang, X. Y.; Chen, E. Y. X. Toward Infinitely Recyclable Plastics Derived from Renewable Cyclic Esters. *Chem* **2019**, *5*, 284–312.
6. Trotta, J. T.; Watts, A.; Wong, A. R.; LaPointe, A. M.; Hillmyer, M. A.; Fors, B. P. Renewable Thermosets and Thermoplastics from Itaconic Acid. *ACS Sustain. Chem. Eng.* **2018**, *7*, 2691–2701.
7. Christensen, P. R.; Scheuermann, A. M.; Loeffler, K. E.; Helms, B. A. Closed-Loop Recycling of Plastics Enabled by Dynamic Covalent Diketoenamine Bonds. *Nat. Chem.* **2019**, *11*, 442–448.
8. Chen, X. S.; Chen, G. Q.; Tao, Y. H.; Wang, Y. Z.; Lv, X. B.; Zhang, L. Q.; Zhu, J.; Zhang, J.; Wang, X. H. Research Progress in Eco-Polymers. *Acta Polym. Sin.* **2019**, *50*, 1068–1082.
9. Chen, Y.-J.; Huang, X.; Chen, Y.; Wang, Y.-R.; Zhang, H.; Li, C.-X.; Zhang, L.; Zhu, H.; Yang, R.; Kan, Y.-H.; Li, S. L. Polyoxometalate-Induced Efficient Recycling of Waste Polyester Plastics into Metal–Organic Frameworks. *CCS Chem.* **2019**, *1*, 561–570.
10. Zhang, X.; Fevre, M.; Jones, G. O.; Waymouth, R. M. Catalysis as an Enabling Science for Sustainable Polymers. *Chem. Rev.* **2018**, *118*, 839–885.
11. Hillmyer, M. A.; Tolman, W. B. Aliphatic Polyester Block Polymers: Renewable, Degradable, and Sustainable. *Acc. Chem. Res.* **2014**, *47*, 2390–2396.
12. Nagarajan, V.; Mohanty, A. K.; Misra, M. Perspective on Polylactic Acid (PLA) based Sustainable Materials for Durable Applications: Focus on Toughness and Heat Resistance. *ACS Sustain. Chem. Eng.* **2016**, *4*, 2899–2916.
13. Auras, R.; Harte, B.; Selke, S. An Overview of Polylactides as Packaging Materials. *Macromol. Biosci.* **2004**, *4*, 835–864.
14. Zhang, L.; Pratt, R. C.; Nederberg, F.; Horn, H. W.; Rice, J. E.; Waymouth, R. M.; Wade, C. G.; Hedrick, J. L. Acyclic Guanidines as Organic Catalysts for Living Polymerization of Lactide. *Macromolecules* **2010**, *43*, 1660–1664.
15. Tang, X.; Chen, E. Y. X. Chemical Synthesis of Perfectly Isotactic and High Melting Bacterial Poly(3-hydroxybutyrate) from Bio-Sourced Racemic Cyclic Diolide. *Nat. Commun.* **2018**, *9*, 2345.
16. Muhammadi; Shabina; Afzal, M.; Hameed, S. Bacterial Polyhydroxyalkanoates-Eco-Friendly Next Generation Plastic:

Production, Biocompatibility, Biodegradation, Physical Properties and Applications. *Green Chem. Lett. Rev.* **2015**, *8*, 56–77.
17. Shi, C.-X.; Guo, Y.-T.; Wu, Y.-H.; Li, Z.-Y.; Wang, Y.-Z.; Du, F.-S.; Li, Z.-C. Synthesis and Controlled Organobase-Catalyzed Ring-Opening Polymerization of Morpholine-2,5-Dione Derivatives and Monomer Recovery by Acid-Catalyzed Degradation of the Polymers. *Macromolecules* **2019**, *52*, 4260–4269.
18. Yu, L.; Zhang, M.; Du, F.-S.; Li, Z.-C. ROS-Responsive Poly(ε-caprolactone) with Pendent Thioether and Selenide Motifs. *Polym. Chem.* **2018**, *9*, 3762–3773.
19. Sanford, M. J.; Van Zee, N. J.; Coates, G. W. Reversible-Deactivation Anionic Alternating Ring-Opening Copolymerization of Epoxides and Cyclic Anhydrides: Access to Orthogonally Functionalizable Multiblock Aliphatic Polyesters. *Chem. Sci.* **2018**, *9*, 134–142.
20. Hu, S.; Zhao, J.; Zhang, G. Noncopolymerization Approach to Copolymers via Concurrent Transesterification and Ring-Opening Reactions. *ACS Macro Lett.* **2015**, *5*, 40–44.
21. Ji, H.-Y.; Wang, B.; Pan, L.; Li, Y.-S. Lewis Pairs for Ring-Opening Alternating Copolymerization of Cyclic Anhydrides and Epoxides. *Green Chem.* **2018**, *20*, 641–648.
22. Hu, S.; Dai, G.; Zhao, J.; Zhang, G. Ring-Opening Alternating Copolymerization of Epoxides and Dihydrocoumarin Catalyzed by a Phosphazene Superbase. *Macromolecules* **2016**, *49*, 4462–4472.
23. Hu, S.; Zhao, J.; Zhang, G.; Schlaad, H. Macromolecular Architectures Through Organocatalysis. *Prog. Polym. Sci.* **2017**, *74*, 34–77.
24. du Boullay, O. T.; Marchal, E.; Martin-Vaca, B.; Cossio, F. P.; Bourissou, D. An Activated Equivalent of Lactide Toward Organocatalytic Ring-Opening Polymerization. *J. Am. Chem. Soc.* **2006**, *128*, 16442–16443.
25. Martin Vaca, B.; Bourissou, D. *O*-Carboxyanhydrides: Useful Tools for the Preparation of Well-Defined Functionalized Polyesters. *ACS Macro Lett.* **2015**, *4*, 792–798.
26. Wang, R.; Zhang, J.; Yin, Q.; Xu, Y.; Cheng, J.; Tong, R. Controlled Ring-Opening Polymerization of *O*-Carboxyanhydrides Using a β-Diiminate Zinc Catalyst. *Angew. Chem. Int. Ed.* **2016**, *55*, 13010–13014.
27. Yin, Q.; Yin, L.; Wang, H.; Cheng, J. Synthesis and Biomedical Applications of Functional Poly(α-hydroxy acids) via Ring-Opening Polymerization of *O*-Carboxyanhydrides. *Acc. Chem. Res.* **2015**, *48*, 1777–1787.
28. Feng, Q.; Tong, R. Controlled Photoredox Ring-Opening Polymerization of O-Carboxyanhydrides. *J. Am. Chem. Soc.* **2017**, *139*, 6177–6182.
29. Feng, Q. Y.; Yang, L.; Zhong, Y. L.; Guo, D.; Liu, G. L.; Xie, L. H.; Huang, W.; Tong, R. Stereoselective Photoredox Ring-Opening Polymerization of *O*-Carboxyanhydrides. *Nat. Commun.* **2018**, *9*.
30. Li, M.; Tao, Y.; Tang, J.; Wang, Y.; Zhang, X.; Tao, Y.; Wang, X. Synergetic Organocatalysis for Eliminating Epimerization in Ring-Opening Polymerizations Enables Synthesis of Stereoregular Isotactic Polyester. *J. Am. Chem. Soc.* **2019**, *141*, 281–289.
31. Kohn, J.; Langer, R. Polymerization Reactions Involving the Side Chains of α-L-Amino Acids. *J. Am. Chem. Soc.* **1987**, *109*, 817–820.
32. Kwon, H. Y.; Langer, R. Pseudopoly(amino acids): A Study of the Synthesis and Characterization of Poly(*trans*-4-hydroxy-N-acyl-L-proline esters). *Macromolecules* **1989**, *22*, 3250–3255.
33. Lim, Y. B.; Choi, Y. H.; Park, J. S. A Self-Destroying Polycationic Polymer: Biodegradable Poly(4-hydroxy-L-proline ester). *J. Am. Chem. Soc.* **1999**, *121*, 5633–5639.
34. Bowers-Nemia, M. M.; Joullié, M. M. A Short Improved Synthesis of N-Substituted 5-aza-2-oxa-3-oxo-bicyclo[2.2.1]heptanes. *Heterocycles* **1983**, *20*, 817.
35. Yuan, J.; Xiong, W.; Zhou, X.; Zhang, Y.; Shi, D.; Li, Z.; Lu, H. 4-Hydroxyproline-Derived Sustainable Polythioesters: Controlled Ring-Opening Polymerization, Complete Recyclability, and Facile Functionalization. *J. Am. Chem. Soc.* **2019**, *141*, 4928–4935.
36. Gui, Y.; Qiu, L. Q.; Li, Y. H.; Li, H. X.; Dong, S. W. Internal Activation of Peptidyl Prolyl Thioesters in Native Chemical Ligation. *J. Am. Chem. Soc.* **2016**, *138*, 4890–4899.
37. Zhao, N.; Ren, C. L.; Li, H. K.; Li, Y. X.; Liu, S. F.; Li, Z. B. Selective Ring-Opening Polymerization of Non-Strained γ-Butyrolactone Catalyzed by A Cyclic Trimeric Phosphazene Base. *Angew. Chem. Int. Ed.* **2017**, *56*, 12987–12990.
38. Bartuschat, A. L.; Wicht, K.; Heinrich, M. R. Switching and Conformational Fixation of Amides Through Proximate Positive Charges. *Angew. Chem. Int. Ed.* **2015**, *54*, 10294–10298.
39. Hinderaker, M. P.; Raines, R. T. An Electronic Effect on Protein Structure. *Protein Sci.* **2003**, *12*, 1188–1194.
40. Hodges, J. A.; Raines, R. T. Energetics of an n→π* Interaction That Impacts Protein Structure. *Org. Lett.* **2006**, *8*, 4695–4697.
41. Yuan, J.; Sun, Y.; Wang, J.; Lu, H. Phenyl Trimethylsilyl Sulfide-Mediated Controlled Ring-Opening Polymerization of α-Amino Acid N-Carboxyanhydrides. *Biomacromolecules* **2016**, *17*, 891–896.
42. Hou, Y.; Yuan, J.; Zhou, Y.; Yu, J.; Lu, H. A Concise Approach to Site-Specific Topological Protein-Poly(amino acid) Conjugates Enabled by *In Situ*-Generated Functionalities. *J. Am. Chem. Soc.* **2016**, *138*, 10995–11000.

DOI: 10.31635/ccschem.020.201900119
CCS Chem. **2020**, *2*, 236–244